Agricultural and Forest Meteorology 354 (2024) 110083

Contents lists available at ScienceDirect

Agricultural and Forest Meteorology

journal homepage: www.elsevier.com/locate/agrformet

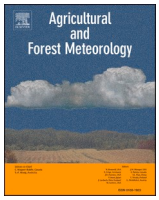

Regional temperature response to different forest development stages in Fennoscandia explored with a regional climate model

Bo Huang [a,*], Yan Li [b], Xia Zhang [a], Chunping Tan [c], Xiangping Hu [a], Francesco Cherubini [a]

[a] Industrial Ecology Programme, Department of Energy and Process Engineering, Norwegian University of Science and Technology (NTNU) N-7491 Trondheim, Norway
[b] Institute of Meteorology, Freie Universität Berlin, Carl-Heinrich-Becker-Weg 6-10 12165 Berlin, Germany
[c] Institute for Disaster Management and Reconstruction, Sichuan University 610200 Chengdu, PR China

ARTICLE INFO

Keywords:
Forest management
Regional climate model
Land cover change
Climate change
Temperature decomposition

ABSTRACT

Several studies investigated the regional temperature effects of afforestation or deforestation, but the impacts of different forest development stages or alternative forest management received limited attention. This is mainly due to challenges in representing area-limited forest dynamics in low-resolution climate models and the need for accurate forest parameters. This study investigates the impact of alternative forest development stages and composition on regional climate in Fennoscandia using a coupled regional climate model. By incorporating realistic and high-resolution forest maps, our modelling framework reduces biases in estimating surface temperature compared to default model runs. If today's forest composition of tree species is left to achieve a mature state (a proxy for the absence of harvesting), an annual mean reduction in 2 m air temperature is estimated, with a cooling peak in summer of -0.53 ± 0.20 °C (mean ± standard deviation) mainly induced by increased cloud cover. Conversely, undeveloped forests (a proxy for increased harvest) induce a contrasting seasonal response: a summer warming of 0.53 ± 0.15 °C (mainly caused by higher sensible heat fluxes), and a weak winter cooling of -0.14 ± 0.24 °C (mainly caused by a higher surface albedo). A transition from evergreen to deciduous forests shows a summer average cooling of -0.57 ± 0.28 °C, mainly attributed to changes in surface albedo. These temperature effects are equivalent to a relatively large fraction of the expected warming by 2050 in Fennoscandia (from 16 % to 70 %, depending on the specific scenario and season). Some modelling outputs appear inconsistent with observations and past modelling studies, such as the cooling effects in winter of more developed forests. Our results provide new insights into the complex relationships between forest dynamics and regional temperature, but modelling improvements are still needed to achieve a robust understanding of the regional climate effects of forest management.

1. Introduction

Forests cover approximately 30 % of the world's ice-free land surface, from tropical to boreal regions (Crowther et al., 2015; Hansen et al., 2013), and play a crucial role in the global carbon cycle (Luyssaert et al., 2018; Pan et al., 2011). They provide a range of ecosystem services, including local-to-regional climate regulation through biogeophysical mechanisms (such as water and heat exchange with the atmosphere) (Anderson et al., 2011; Bonan, 2008). At fine local scales, forest growth and management primarily induce changes in microclimatic conditions, such as those from alterations in shade effects and exposure of forest understory to solar radiation from variations in forest canopy and density (De Frenne et al., 2021, 2019; Haesen et al., 2023). At a regional level, the climate effects of forests depend on their structure and composition, and are dependant on the forest development stage and management (Kellomäki et al., 2021; Kumkar et al., 2020; Luyssaert et al., 2014; Naudts et al., 2016). Forest disturbances for timber harvest can directly impact surface albedo by altering land surface cover (Doughty et al., 2018; Luyssaert et al., 2018). Changes in albedo modify the balance of incoming solar radiation and outgoing longwave radiation, subsequently influencing regional temperature patterns and surface energy fluxes (Betts, 2000). The evapotranspiration process in forests, whereby plants release water vapour into the atmosphere through transpiration and evaporation from soil and canopy surfaces, also regulates the regional climate (Komatsu and Kume, 2020). Forest management can modify evapotranspiration rates, affecting

* Corresponding author.
E-mail address: bo.huang@ntnu.no (B. Huang).

https://doi.org/10.1016/j.agrformet.2024.110083
Received 13 October 2023; Received in revised form 21 May 2024; Accepted 24 May 2024
Available online 29 May 2024

humidity levels (Ellison et al., 2017; Wei et al., 2022). This can influence cloud cover and moisture recycling, potentially leading to changes in local and regional precipitation patterns. Additionally, altered forest structures induced by management practices can lead to variations in surface roughness (Winckler et al., 2019) and exert an influence on wind patterns and turbulence, thereby affecting boundary layer dynamics and subsequently shaping the regional climate (Venäläinen et al., 2004).

Forests are heavily managed in Fennoscandia (i.e., Norway, Sweden, and Finland), primarily via rotation forestry (Petersson et al., 2022; Zhou et al., 2021). Harvest disturbances change various forest structural attributes, including tree density, standing volume, leaf area index, crown length, and canopy height (Anderson et al., 2011; Jackson et al., 2008). These attributes control surface energy, moisture, and momentum fluxes, which have a significant impact on regional climate through surface albedo, evapotranspiration, and surface roughness (Anderson et al., 2011; Jackson et al., 2008). However, the representation of various forest development stages in existing land surface models is limited. Typically, the same parameterization of leaf area index or canopy height is used for different vegetation classes and ages, irrespective of forest development stage or age (Lawrence et al., 2019). Although efforts have been made to embed different forest stage parameterizations within gridded land use datasets for various forest types (Majasalmi et al., 2018; McGrath et al., 2015), linking forest dynamics with climate models remains complex, limiting the applicability of such models (Kumkar et al., 2020; Luyssaert et al., 2018; Naudts et al., 2016).

Global climate models, with their coarse spatial resolutions and uncertainties in physical processes, are unsuitable for studying the impacts of forestry on regional climate and the changes induced by small-scale management disturbances. Although regional climate models can achieve a finer resolution, they still face challenges in simulating the complex spatial and temporal patterns of forest dynamics, and their simulated response to land cover changes is often contradictory (Davin et al., 2020; de Noblet-Ducoudré et al., 2012). The availability of accurate spatial datasets of forest composition and structural attributes can also be a limitation, as deriving these datasets requires regression analysis based on long timeseries of on-site measurements and remote-sensing data. Once available, they can enhance the representation of forest attributes in climate models and potentially improve the possibilities to capture the regional climate impact of forest dynamics. This can lead to improved model simulations within climate models and a better understanding of the complex interactions between the land surface and the atmosphere, ultimately enhancing our ability to predict and mitigate the effects of climate change or optimize management practices.

Forest management interacts with the climate system via biogeophysical and biogeochemical (i.e. changes in the carbon cycle) mechanisms. In terms of the biogeophysical effect, Naudts et al. (2016) used a land-atmosphere model to analyse the historical impacts of forest management in Europe, revealing a 0.12 °C average increase in summertime atmospheric temperature due to the widespread conversion of broadleaf to coniferous trees (which have higher timber values). More specifically to Fennoscandia, Kumkar et al. (2020) conducted offline simulations with a land surface model, showing that older forests induce a slight cooling while younger forests tend to warm the surface. Huang et al. (2023a) applied a series of machine learning algorithms to datasets of forest structural attributes and satellite retrievals of land surface temperature and found that older forests are generally warmer than younger forests, except for the summer. Both Kumkar et al. (2020) and Huang et al. (2023a) lacked consideration of energy and mass feedbacks between the land surface and the atmosphere, which is a main constraint to determine the temperature impacts of forest dynamics and management.

The goal of this study is to assess how a regional climate model (RCM) enhanced with a land cover dataset with highly parameterized forest composition and structure can simulate the effects on regional climate of alternative forest development stages and tree composition. This is an attempt to close the existing gap between structural and compositional variety of forests and the climate modelling framework, with the ambition to gain new insights into how the surface energy balance of boreal forests is affected by structural perturbations. More specifically, the aims of the study are the following: (1) estimate if a RCM can improve the representation of 2 m (2 m) air temperature and land surface temperature when an advanced land cover dataset with more parameterized forest attributes is used instead of default land cover data; (2) evaluate, across different temporal and spatial scales, the sensitivity of 2 m air temperature and land surface temperature to idealized changes in forest structure and composition that resemble alternative forest development stages and management strategies; (3) assess the key drivers of the changes in the land surface temperature through a decomposition analysis.

2. Methods

2.1. Datasets used for model validation

The performance of the model in capturing near surface air temperature is evaluated by validating model outputs against monthly means of 2 m air temperature from the E-OBS datasets (Cornes et al., 2018). E-OBS is an observational dataset that provides daily gridded land-only data over Europe. The dataset includes a blend of time series obtained from the station network of the European Climate Assessment & Dataset project. To assess the model's ability to replicate land surface temperature, data from ERA5-Land datasets (Muñoz-Sabater et al., 2021) are used. The ERA5-Land dataset is a reanalysis of land variables, offering consistent information on land surface temperature evolution over several decades. With a resolution of approximately 9 km (0.1° × 0.1°), ERA5-Land combines observations with model data to create a globally complete and coherent dataset. To prevent model-based estimates from deviating too far from actual conditions, ERA5-Land adjusts the input air temperature, humidity, and pressure for the altitude differences between the forcing grid and the higher-resolution ERA5-Land grid through a lapse rate correction.

The E-OBS and ERA5-Land datasets integrate multiple sources of information (field measurements, remote sensing and modelling/interpolation) and are typically chosen as observational data to validate climate model outputs due to their robustness and extensive area coverage. In regional climate model simulations, the land surface temperature indicates the combined temperature of surface components (including both the ground and the vegetation cover), meaning that it is the temperature above the canopy when the grid is covered by forests. In contrast, the near-surface air temperature is traditionally defined as the 2 m air temperature, and it is situated below the canopy if the grid is covered by tall trees. As ERA5's land surface temperature and E-OBS's air temperature assume an unforested surface as they are mainly extrapolated from weather stations that are typically located outside forests, some discrepancies between model simulations and observations may occur. Both the E-OBS and ERA5-Land datasets were subjected to bilinear interpolation onto our model simulation grids, and were averaged over the period 2012–2015 to align with model simulations. Indices like the pattern correlation coefficient (PCC), the regional mean bias (BIAS), and the root-mean-square error (RMSE) were used for model validation (see Supplementary Text 1 in the Supplementary Information).

Future temperature projections for 2050 (as ten-years mean 2046–2055) are used to benchmark the temperature effects of the forest development scenarios described below. They were obtained at a grid resolution of 0.11° from the ensemble mean of CORDEX regional climate models for two Representative Concentration Pathways (RCPs): RCP2.6 (corresponding to a global average temperature increase of 0.9–2.3 °C by 2100) and RCP4.5 (1.7–3.2 °C). RCP8.5 is excluded because is usually considered to induce an excessive warming level that is inconsistent with current emission trajectories (Hausfather and Peters, 2020), and

RCP6.0 because of a lack of model outputs for this scenario in the CORDEX dataset. The details of the considered model simulations are available in Table S1. For each scenario, the multi-model mean of the temperature change was calculated from 12 simulations for RCP2.6 and 13 simulations for RCP4.5, relative to 2010 (intended as a ten-year mean 2006–2015).

2.2. Enhanced land cover dataset with improved forest parameterization

Forest structure parameters were derived from an improved land cover dataset created to represent forest conditions in Fennoscandia (Majasalmi et al., 2018). This dataset was integrated into the European Space Agency Climate Change Initiative Land Cover (ESA CCI LC) map (ESA, 2017), where the forest classes are updated with attributes from National Forest Inventory data from 2015. The dataset identifies the three main tree species in the region (two evergreen species, pine and spruce, and one deciduous, birch) and provides information on various structural attributes for each species in four different forest development stages. Forest areas are grouped into four classes, ranging from a forest with predominately young or less developed trees, as commonly found in post-harvest sites and early successional forest, to a forest with a well-developed tree structure and canopy, indicative of low management intensity or mature secondary forests. Attributes such as total stem volume, maximum growing season leaf area index, tree crown length, and mean tree Lorey's height (i.e., the basal-area-weighted mean tree height) are available for each tree species and development class. Although the definition of the different classes is to a large extent generic, it differentiates between tree species and between forest development stages, and it is based on observed physical characteristics of the forest. This is a considerable improvement relative to default datasets typically used in RCMs, which assign a forest to a single class (e.g., evergreen needleleaf forest or broadleaf deciduous forest) whose parameterization is standardized without any further distinction of age or vegetation structure. The time-invariant nature of the fixed parameterization in each forest class is here avoided by increasing the number of classes for the same type of forest with a differentiation in key structural attributes (i.e., from young to mature forests). By prescribing changes amongst forest classes, it thus becomes possible to explore with a climate model the effects of alternative forest development stages on the regional climate.

To better represent forest characteristics and facilitate their integration into the RCM, some changes have been made to this dataset. Pine and spruce trees have been grouped into one forest class (evergreen forests) and birch trees have been categorized as deciduous forests. In order to optimize the computational time and reduce the need to create new land cover classes, three development classes (DC) have been created out of the four available in the original dataset: DC1 for young or less developed trees, DC2 for middle-developed trees, and DC3 for well-developed trees. Here, DC2 includes classes 2 and 3 from the original classification by Majasalmi et al. (2018). To assign forest attributes like leaf area index, tree crown length, and mean tree Lorey's height to different forest types and development classes, the averages of these attributes have been calculated for relevant trees (Table S2). For evergreen forest DC1, the average attributes of class 1 for spruce and pine are considered, while evergreen forest DC2 is the average of the attributes of spruce and pine for classes 2 and 3. Evergreen forest DC3 corresponds to the average attributes of class 4 for spruce and pine. The same approach has been followed to assign forest attributes for deciduous forest. The enhanced land cover dataset with improved forest parameterization is only used inside Fennoscandia. Our simulation domain includes some bordering areas for which the default land cover classes (i.e., the ESA CCI LC) are used and are not affected by the simulated transitions discussed below. Both the enhanced land cover and the default dataset have been aggregated to align with the model simulation grid (5 km), thus harmonizing the distribution of land cover across the domains.

2.3. Regional climate model

The Weather Research and Forecasting (WRF) model version 4.3 was used for regional climate simulations, which is a state-of-the-art mesoscale model suitable for operational research across scales (Skamarock et al., 2021). The model uses actual atmospheric conditions based on observations and analyses, and has been validated against observations in Europe to accurately capture spatiotemporal climate patterns (Katragkou et al., 2015; Kotlarski et al., 2014). WRF has also been utilized in investigating the interaction between land cover changes and climate variability in Europe (Huang et al., 2020; Mooney et al., 2020). In regional climate models, mesoscale processes do not interact with the global climate, and large-scale feedbacks that depend on these interactions are not properly represented. However, many important feedbacks operate at the local scale, such as the snow-albedo feedback, and these are captured by RCM simulations.

In this study, the model simulations were based on the EURO—CORDEX configuration in the first domain (Domain 1) and a one-way nested simulation over Northern Europe (Domain 2). The simulations have an approximate spatial resolution of 15 km within the first domain (Domain 1, comprising 346 × 290 grids) and 5 km within the inner domain (Domain 2, consisting of 351 × 393 grids). The initial and lateral boundary conditions were obtained from the European Centre for Medium-Range Weather Forecasts (ECMWF) fifth reanalysis (ERA5) (Hersbach et al., 2020). The model employed physical parameterization schemes such as the Thompson microphysics scheme (Thompson et al., 2008), the Rapid Radiative Transfer Model for longwave and shortwave radiation (Iacono et al., 2008), the Mellor-Yamada Nakanishi and Niino boundary layer scheme (Nakanishi and Niino, 2006), and the Kain-Fritsch convection parameterization (Kain, 2004). All simulations were conducted for the period 2011–2015. The first year is considered a spin-up time and excluded from the subsequent analysis.

WRF is coupled to the Community Land Model version 4.0 (CLM4) to simulate land surface processes, with the International Geosphere-Biosphere Programme (IGBP) – Moderate Resolution Imaging Spectroradiometer (MODIS) land use classification (Lawrence et al., 2011; Oleson et al., 2010). CLM4 is a comprehensive land surface process model that includes components related to land biogeophysics, hydrologic cycle, biogeochemistry, human dimensions (i.e., land use, agriculture, urbanization), and ecosystem dynamics. The model incorporates a single-layer vegetation canopy, a five-layer snowpack, and a ten-layer soil column with a detailed description of the land surface, including surface heterogeneity (Skamarock et al., 2021). The land surface is categorized into five primary subgrid land units, each with unique characteristics that share the same atmospheric forcing and flux feedback within a grid cell. The urban land unit is represented by the "urban canyon" concept (Oke, 1987), while the vegetated subgrid comprises up to 15 plant functional types (PFTs) with different optical, physiological, and aerodynamic properties. The PFTs' parameters are prescribed monthly and updated daily using linear interpolation (Lu and Kueppers, 2012). CLM4 includes new treatments of soil column-groundwater interactions, soil evaporation, and snow cover fraction, amongst others. The model equivalent surface albedo is calculated using monthly soil moisture and PFT parameters. The energy balance and surface fluxes are calculated at the PFT level before being aggregated at the grid-scale level based on the proportion of PFTs in the grid cell. A simulation was initiated employing the default IGBP-MODIS land use classification (referred to as DEFAULT). This simulation serves as a basis for contrasting the model's performance with a novel land use classification derived from an enhanced land cover dataset.

In order to enable WRF to read the enhanced land cover dataset, the latter has to be converted from the ESA CCI LC classification to the IGBP-MODIS classification system via a cross-walking table (Table S3), and then to PFTs (Table S4), in line with the approach used in other studies (e.g., Duveiller et al. (2018) and Huang et al. (2020)). In this study, we have further redefined the IGBP-MODIS classification system by

introducing three new classes to represent the three alternative development classes for evergreen forest and deciduous forest discussed above, with their respective forest structure attributes. These new classes are used to simulate forest transitions and management. These classes are then associated with different parameterizations by alternative PFTs, for which the forest characteristics explained above (i.e., leaf area index, crown length, and canopy height) are modified according to the specific development class (the other forest-based parameters are kept the same) (Table S5).

2.4. Scenarios of alternative forest development stages and tree composition

The enhanced dataset that provides an observation-based representation of the current structure and composition of Fennoscandian forests is utilized to set the present condition of the forest and to establish a control experiment (CONTROL). To analyse the potential impacts of different states of the forest, we consider three alternative scenarios of forest development stages and composition that cover the breadth of the possible changes affected by alternative management systems: undeveloped forests (undevelopedF), fully developed forests (developedF), and a forest transition from spruce or pine forests to birch dominated forests (moredecidF). These scenarios have been designed in light of the main contrasting approaches that are frequently discussed for changing the management of boreal forests for better contributing to climate change mitigation and/or nature conservation, i.e. increase harvesting (undevelopedF), reduce harvesting to maximize vegetation carbon stocks (developedF), or to promote regeneration of naturally occurring deciduous species to support nature conservation (moredecidF) (Ameray et al., 2021; Högberg et al., 2021; Mäkelä et al., 2023).

In undevelopedF, all grid cells covered by forests in CONTROL are converted to DC1 of the corresponding tree type (either evergreen forest or deciduous forest), which is the least developed class. This is implemented across all tree species in all forested regions of Fennoscandia. This scenario can be considered as a proxy to simulate a situation where only low-developed and/or early successional forests are present, reflecting major losses in standing forest stocks or effects of clear-cut harvesting.

In developedF, all grid cells where forests are dominant in CONTROL are converted to DC3 of the corresponding tree type, which corresponds to the most developed forest class. This case is indicative of an idealized situation where there is no or limited forest harvest, as all forests are at their mature state (characterized by the highest leaf area index, canopy height etc.). It can be interpreted as representative of a strategy aiming at maximizing forest carbon stocks through no harvest and/or avoidance of clear-cut, fertilization, increased plant density, etc.

In both undevelopedF and developedF scenarios, the forest composition remains unaffected, and only the structural attributes are changed. In moredecidF, a change in tree composition is modelled. All grid cells where evergreen forest cover is dominant in CONTROL are converted to the same deciduous forest class, so to explore the effects of a tree species change. This scenario can be interpreted as a strategy that favours the natural regrowth of deciduous species to co-promote vegetation carbon storage and nature conservation, as deciduous species are usually of higher value for biodiversity than artificially planted evergreen species like spruce and pine (which in turn have higher timber value than birch).

In each scenario, the land cover datasets include modifications in land surface parameters corresponding to different forest development stages that are amongst the key drivers of variations in the surface energy balance. For instance, LAI affects the amount of water intercepted by the vegetation and it directly influences surface albedo and how energy fluxes are partitioned between sensible and latent heat, or canopy height can affect the turbulent mixing of heat in the atmosphere as it determines roughness length. The changed parameters remain constant during the entire simulation period to enhance the model response.

2.5. Decomposition of the surface energy balance

The surface energy balance is a complex interplay between various biogeophysical properties of the surface, including surface albedo, ground heat conductance, and partitioning of turbulent heat fluxes. The land surface temperature (LST) is derived from emitted longwave radiation according to the Stefan-Boltzmann law as described in Oleson et al. (2013). To understand the most important drivers of LST changes induced by forest management scenarios, we performed a decomposition analysis where we attribute the differences in simulated LST (ΔLST) between the three scenarios and CONTROL to the underpinning variations in surface energy/moisture fluxes and albedo (Luyssaert et al., 2014; Winckler et al., 2019). The analysis aims to explore the relationship between temperature changes and variations in specific components of the surface energy budget, elucidating the influence of simulated modifications in forests. The method can be expressed through the following equation:

$$\Delta LST = \frac{1}{f}\left(- Rsi\Delta\alpha + (1-\alpha)\Delta Rsi + \Delta Rli - \Delta\lambda E - \Delta H - \Delta G - \Delta I - \sigma LST^4\Delta\varepsilon\right) \quad (1)$$

$$f = 4\varepsilon\sigma LST^3 \quad (2)$$

The change in land surface temperature (ΔLST) resulting from land management changes are thus decomposed into eight factors. The symbol Δ represents the difference between two simulations for each variable in each grid cell. The term $\frac{-Rsi\Delta\alpha}{f}$ represents the contribution of change in albedo (α), with a negative $\Delta\alpha$ indicating that the albedo has decreased (the surface is darker) following forest cover change, resulting in more absorption of incident shortwave radiation, and then leading to a warming surface (positive ΔLST). $\frac{(1-\alpha)\Delta Rsi}{f}$ represents the change in incoming shortwave radiation (Rsi), with a positive ΔRsi indicating that the new land cover receives more incoming shortwave radiation than the initial land cover (e.g., due to a change in cloud cover from increased evapotranspiration), implying a warming surface. $\frac{\Delta Rli}{f}$ represents the contribution of incoming longwave radiation (Rli) in LST change, with a positive ΔRli indicating an increase in incoming longwave radiation from the atmosphere, and then leading to a positive ΔLST. $\frac{-\Delta\lambda E}{f}$ shows the change in latent heat flux (λE) impacting on ΔLST, with a positive $\Delta\lambda E$ indicating that the new land cover/management has more evaporative cooling than the original land cover/management, conducting a cooling land surface. $\frac{-\Delta H}{f}$ shows the change in sensible heat flux (H) contributing to the ΔLST, with a positive ΔH indicating a cooling land surface, similar to changes in λE. $\frac{-\Delta G}{f}$ shows the contribution of soil heat flux (G), also similar to changes in λE. $\frac{-\Delta I}{f}$ represents the effect of the change in residual flux, which combines unmeasured fluxes and measurement errors of the observed fluxes. Finally, $\frac{-\sigma LST^4\Delta\varepsilon}{f}$ presents the change in the thermal emissivity of the surface, with a positive $\Delta\varepsilon$ indicating that the new land cover emits more outgoing longwave radiation due to its higher emissivity coefficient, resulting in a lower LST. Surface emissivity is closely related to vegetation canopy density. As forest harvest reduces canopy density, it tends to decrease surface emissivity and, consequently, results in a warmer surface. The symbol f refers to the energy redistribution factors for surface temperature.

The decomposition approach offers the advantage of quantifying the overall impact of dynamic responses. For instance, if forest management leads to a decrease in LAI, the soil heat flux is likely to increase, resulting in less available energy for latent and sensible heat fluxes, assuming all other factors remain constant. However, the change in LAI also alters surface net radiation, which depends on the modified surface albedo and temperature. The decomposition approach captures the net effect of the decrease in LAI. Nevertheless, this approach does not measure the gross

fluxes for the above example, i.e., how much of the change in latent heat is due to the change in LAI, in net radiation, or the change in the temperature gradient between the canopy and the atmosphere.

3. Results

3.1. Current forest structure and composition

In Fennoscandia, forests cover more than 60 million hectares, or 57 % of the land area. Norway, Sweden, and Finland have a forest coverage of about 30 %, 68 %, and 73 %, respectively, with pine being the most common tree species, followed by spruce and birch. According to our enhanced land cover dataset with forest structure parameterization, spruce or pine at development class 2 (DC2) is the current dominant land cover in Fennoscandia (Fig. 1a). Spruce or pine DC1 covers a larger area than DC3, primarily due to historical intensive forest management activities (Iordan et al., 2018; Zhou et al., 2021). Deciduous species like birch, occasionally mixed with other species (e.g. Acer, Fagus, Quercus), are primarily associated with natural forest succession or early-stage tree encroachment. Evergreen needleleaf forest (unclassified), croplands, and open shrublands are the most abundant outside Fennoscandia (Fig. 1f). Fig. 1b, 1d, and 1e show the changes simulated in the dominant land cover distributions in the forest management scenarios.

As the regional climate model only considers the dominant land cover per grid cell, the area per land cover class in Fennoscandia accounting for the fraction in each grid cell vs. the area estimated when only the dominant land cover type is considered are compared in Fig. 1c. This shows the extent by which the model limitation to read only the dominant land cover class per grid cell deviates from the real distribution of land cover classes as fractions of each grid cell. For example, considering the fractions in each grid, spruce or pine DC2 occupy an area of around 65 Mha. If we only consider the dominant land cover type in each grid, the area occupied by spruce or pine DC2 decreases to around 40 Mha. amongst the forest development classes of interest, the area occupied by spruce or pine DC3 when accounting only for the grids where they are the dominant land cover is less than that obtained by summing the respective land cover fractions per grid. On the other hand, the less developed forest classes spruce or pine DC1 cover a larger area, from around 7 to 14 Mha. Additionally, all classes of birch-dominated forests (birch dominated DC1 to DC3) show a larger area compared to the sum of land cover fractions. This indicates the mixes of forest classes in the various grid cells, as a result of small-scale management interventions that have historically affected forest areas in Fennoscandia. While these practices did not involve the complete clearance of forests at the grid-level resolution, they led to the mixing of different forest classes in the research domain.

3.2. Validation of regional climate projections with the enhanced forest dataset

The performances of the model simulations with the enhanced forest cover datasets (CONTROL) in reproducing the European climate are compared with those from a default experiment (DEFAULT) based on the conventional land cover dataset. Both the DEFAULT and CONTROL simulations show a cooling bias in the annual mean 2 m air temperature, as shown in Fig. 2a and 2b. However, the WRF model with the new forest cover classification (i.e., CONTROL) has a reduced bias compared to the DEFAULT simulation (−1.40 °C vs. −1.87 °C). The largest bias between model simulations and observations is located over the mountains along the Norway-Sweden border and in western Norway. The CONTROL simulation exhibits an overall reduced bias, especially in the central-to-northern part (Sweden and Finland). The probability density function

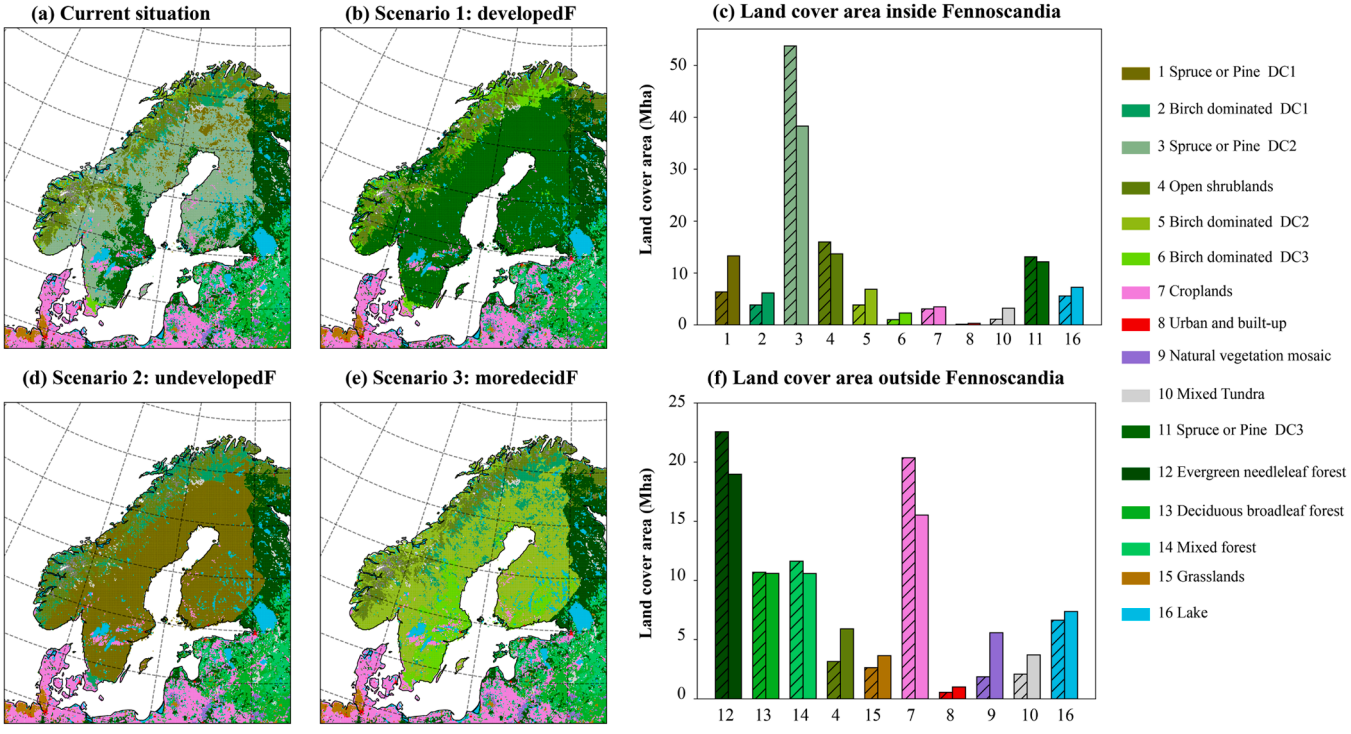

Fig. 1. Distribution of land cover types within Fennoscandia and the nearby areas included in the simulation domain. The dominant land cover types are shown for the current land cover (CONTROL; a) and for the investigated forest management scenarios: fully developed forests (developedF; b), undeveloped forests (undevelopedF; d), and forest transitions from spruce or pine forests to birch-dominated forests (moredecidF; e). The bar chart shows the land cover area per each class in the CONTROL simulation inside (c) and outside (f) Fennoscandia, represented by considering either the fraction of each land cover type in every grid (indicated by the colour bar with hatch) or the dominant land cover type in each grid (indicated by the full colour). The difference between the bars indicates the approximation done in the climate model simulations, where only the dominant land cover type is considered. Forests without an indication of development class (e.g., evergreen needleleaf forest, mixed forest, etc.) are generic classes, and are only present outside Fennoscandia.

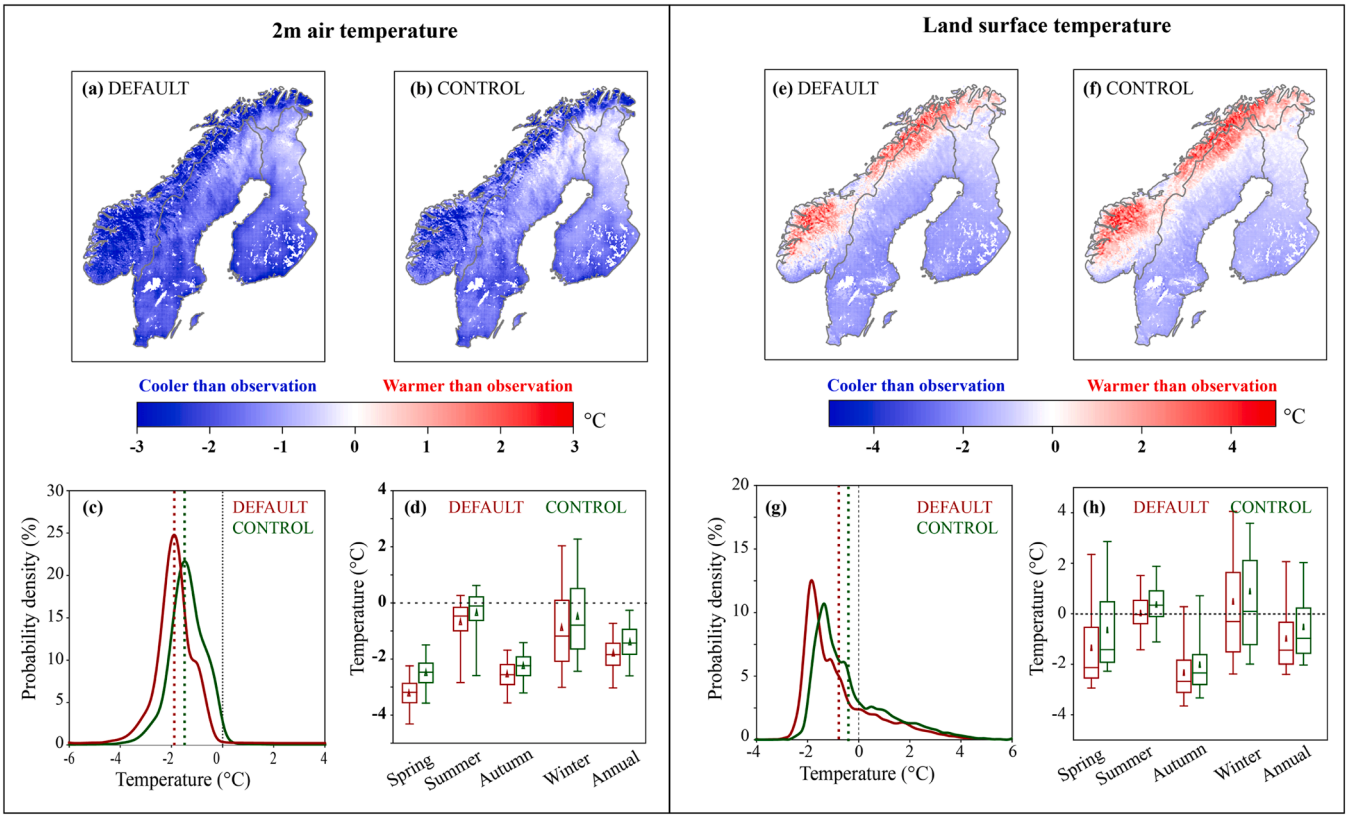

Fig. 2. Performance of WRF model simulations based on either a default (DEFAULT) or an enhanced forest cover dataset (CONTROL) against observations. Both 2 m air temperature (left panel) and land surface temperature (right panel) are considered for validation. (a) and (b) show the difference in annual mean 2 m air temperature (unit: °C) between model simulations and observations in the DEFAULT and CONTROL, respectively. (c) presents a probability density plot showing the distribution of the difference in annual mean 2 m air temperature (unit: %). Boxplots show the annual mean and seasonal mean 2 m air temperature changes (unit: °C, d); the range represents the 5th and 95th percentiles, the box is the standard deviation, the line is the median and the triangle is the average. (e-h) are the same as (a-d), but for the land surface temperature. The E-OBS dataset serves as the observational dataset for 2 m air temperature, while the ERA-Land is the observational dataset for land surface temperature.

distribution shows that the difference between the simulated and observed 2 m air temperature resembles a Gaussian distribution for both DEFAULT and CONTROL simulations (Fig. 2c). The majority of the temperature differences are clustered around the mean with a symmetric pattern, and confirm the improved model performance achieved with the new land cover classification. The cooling bias of both simulations occurs in all seasons, but it is generally smaller in the CONTROL simulation than in the DEFAULT simulation (Fig. 2d). All grids are cooler in the CONTROL simulation than observations during spring and autumn, with a range of −3.43/−1.38 °C and −3.17/−1.36 °C (as 5th/95th percentile), respectively. However, some grids show a warming bias in summer and winter, with biases up to 0.66 °C and 2.34 °C, respectively.

WRF model simulations with the new forest cover classification also reduce the bias of land surface temperature (Fig. 2e-2h). The annual mean bias shows some positive values at high elevations for both simulations (Fig. 2e and 2f). The CONTROL simulation shows an overall improvement in model performance, as confirmed by the annual mean bias (−0.79 vs. −0.33 °C for DEFAULT and CONTROL, respectively) and the probability density function distribution of the difference between simulated and observed values (Fig. 2g). The improvement in model performance also occurs throughout the seasons (Fig. 2h). In comparison to the DEFAULT simulation, the CONTROL simulation has a comparable pattern correlation coefficient, while concurrently achieving a consistent reduction in the root-mean-square error across all seasons (Table S6).

3.3. Temperature effects of alternative forest scenarios

The WRF model with the enhanced forest cover dataset is used to assess the temperature changes resulting from three alternative scenarios of forest development stages and composition (developedF, undevelopedF, moredecidF) in Fennoscandia (Fig. 3). If all forests in the region are at a mature and developed stage DC3 (developedF), the annual average 2 m air temperature would experience a cooling of −0.21 °C (−0.40/−0.05 °C as 5th/95th percentile) for the entire Fennoscandia, and −0.25 °C (−0.42/−0.10 °C) on the grids affected by the forest structural change (Fig. 3a). The cooling effect is consistently spread across the domain, and it is mostly pronounced in central-northern Sweden, where there is a high concentration of poorly developed forest (DC1 and DC2) that is replaced by more structured forest (DC3). The statistical distribution of the changes in annual mean 2 m air temperature has a gaussian distribution, with a peak at about −0.25 °C (Fig. 3d). The statistics for the developedF scenarios produced from the WRF simulations are shown in Supplementary Table S7. The cooling effect is mainly seen in the summer season, with a regional cooling of −0.49 ± 0.20 °C (mean ± standard deviation), or −0.53 ± 0.20 °C in the grids with forest changes only (Figure S1b). Results are more scattered in spring and autumn, while a temperature reduction is also observed in winter. This winter cooling effect (−0.22 ± 0.14 °C in grids with forest change) in the developedF is difficult to explain, and it is discussed in more detail in the section on the decomposition analysis.

The undevelopedF scenario simulates a situation where all forests in Fennoscandia are at a low development stage (DC1), and it is associated with a predominant annual 2 m air temperature warming of 0.28 ± 0.18

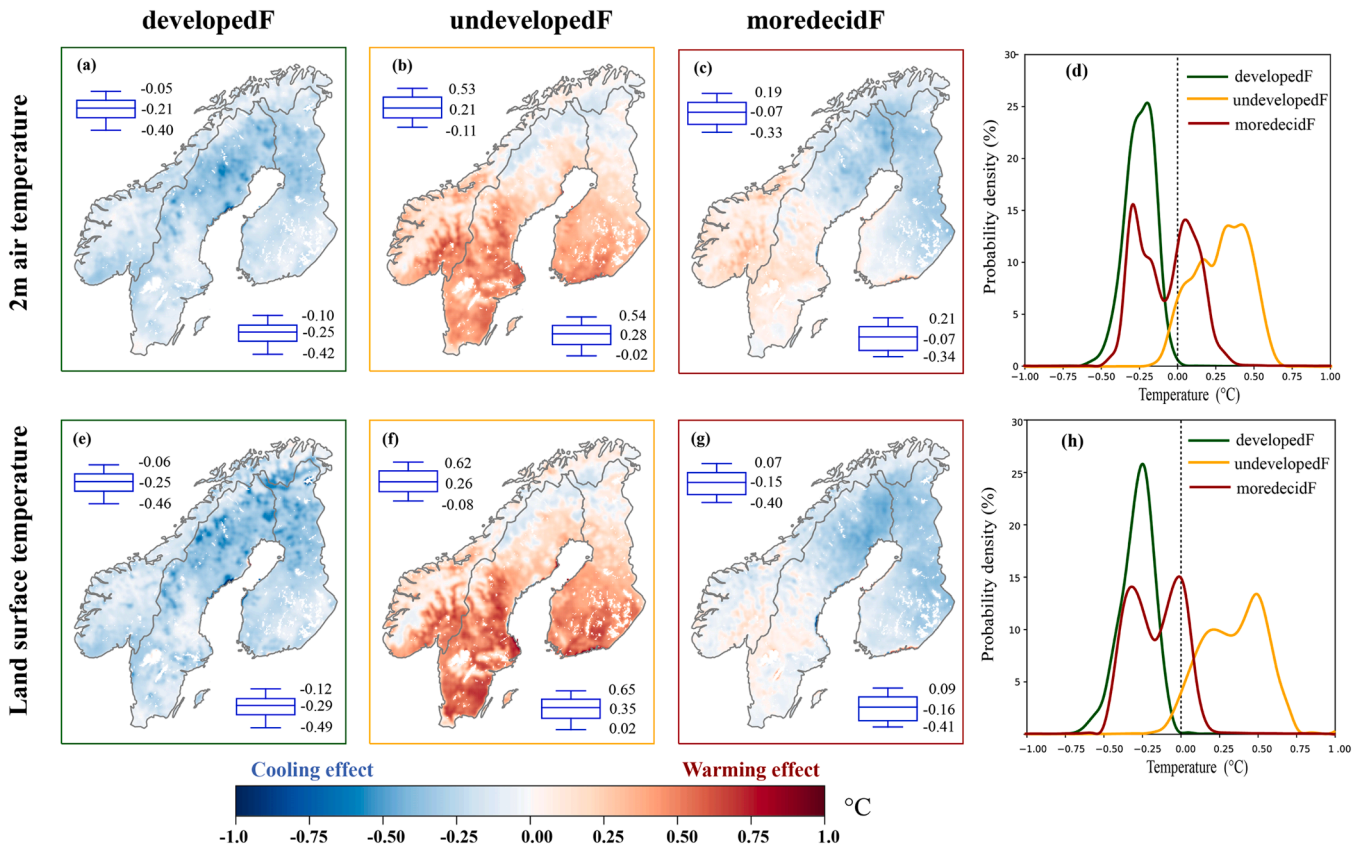

Fig. 3. Changes in near surface 2 m air temperature (upper row) and land surface temperature (lower row) induced by the investigated forest scenarios. Annual mean 2 m air temperature differences between: (a) a scenario with full development class (DC3) of all forested areas and present-day forests (developedF – CONTROL); (b) all undeveloped forests (DC1) and present-day forests (undevelopedF – CONTROL); (c) transition from evergreen forests to deciduous forests and present-day forests (moredecidF – CONTROL). Probability density distribution (in %) of difference in annual average 2 m air temperature between simulated scenarios and present-day (d). Annual mean land surface temperature differences between: (e) a scenario with full development class (DC3) of all forested areas and present-day forests (developedF – CONTROL); (f) all undeveloped forests (DC1) and present-day forests (undevelopedF – CONTROL); (g) transition from evergreen forests to deciduous forests and present-day forests (moredecidF – CONTROL). Probability density distribution (in %) of differences in annual average land surface temperature between the simulated scenarios and present-day (h). The boxplots are based on the average regional 2 m air temperature/land surface temperature change for each simulation (the range indicates the 5 % and 95 % percentile values, the box the standard deviation, and the line the mean). The colour of the boxes around the maps corresponds to the colors of the management scenarios in the probability density distributions.

°C (with a range of −0.02–0.54 °C as the 5th-95th percentile) (Fig. 3b). Several grids experience warming that can be up to 1.0 °C (especially in the southern part of the domain), while others in the north show a light cooling effect (around −0.1 °C). The statistical distribution of changes in annual mean 2 m air temperature shows a predominant abundancy of positive changes, with a peak at about 0.3–0.5 °C (Fig. 3d). The induced temperature effect shows a strong seasonality, with significant regional warming in summer (0.41 ± 0.19 °C) (Figure S1f). This warming effect is more pronounced in the grids with forest changes (0.53 ± 0.15 °C). We can also observe regional warming in most grids in spring and autumn, with average temperature increases of 0.43 ± 0.29 °C and 0.31 ± 0.21 °C, respectively. In contrast, there is cooling in winter (−0.19 ± 0.24 °C), caused by more exposed snow surfaces in younger forests (higher albedo, Figure S2) and therefore more reflected sunlight. Supplementary Table S7 provides the statistics regarding the undevelopedF scenarios generated from the WRF simulation.

Converting all evergreen forests to deciduous forests (moredecidF) at their respective development level leads to a slight regional annual cooling (−0.07 ± 0.18 °C) in Fennoscandia (Fig. 3c). There is an evident spatial variability in the temperature effect, with a slight warming in the southwest and a cooling in the northeast. The statistical distribution of 2 m air temperature changes has two peaks, one at about 0.02 °C and another at about −0.35 °C (Fig. 3d). A similar contrast in the temperature response is also observed in spring, autumn, and winter (Figure S1i, S1k, and S1l), while there is a significant cooling effect in summer with a regional mean of −0.47 ± 0.32 °C and an effect on the involved forest grids of −0.57 ± 0.28 °C (Figure S1j).

When considering the effects of forest management on land surface temperature, we observe changes that have the same sign as those in 2 m air temperature, but the magnitude is more pronounced (Fig. 3e-3g). For instance, in the developedF scenario, the annual mean changes are −0.25 ± 0.13 °C for the regional mean (vs. −0.21 ± 0.11 °C for the 2 m air temperature) and −0.29 ± 0.13 for affected grids only (vs. −0.25 ± 0.11 °C for the 2 m air temperature). The statistical distribution of land surface changes induced by forest management shows a similar shape to that of the 2 m air temperature (Fig. 3h). Like the 2 m air temperature, the changes in land surface temperature also have strong seasonality (Fig. 4). A significant cooling effect in summer can be found in the developedF and moredecidF scenarios, while a warming summer is observed in the undevelopedF scenario. The cooling effect in summer is more substantial in the developedF than in the moredecidF scenario, with values of −0.71 ± 0.28 °C and −0.61 ± 0.32 °C, respectively. The median warming summer in undevelopedF is 0.91 °C, with a range of 0.50–1.22 °C as the 5th-95th percentile, averaged across the affected grids. The statistics of changes in land surface temperature induced by developedF, undevelopedF, and moredecidF scenarios are shown in Supplementary Table S7.

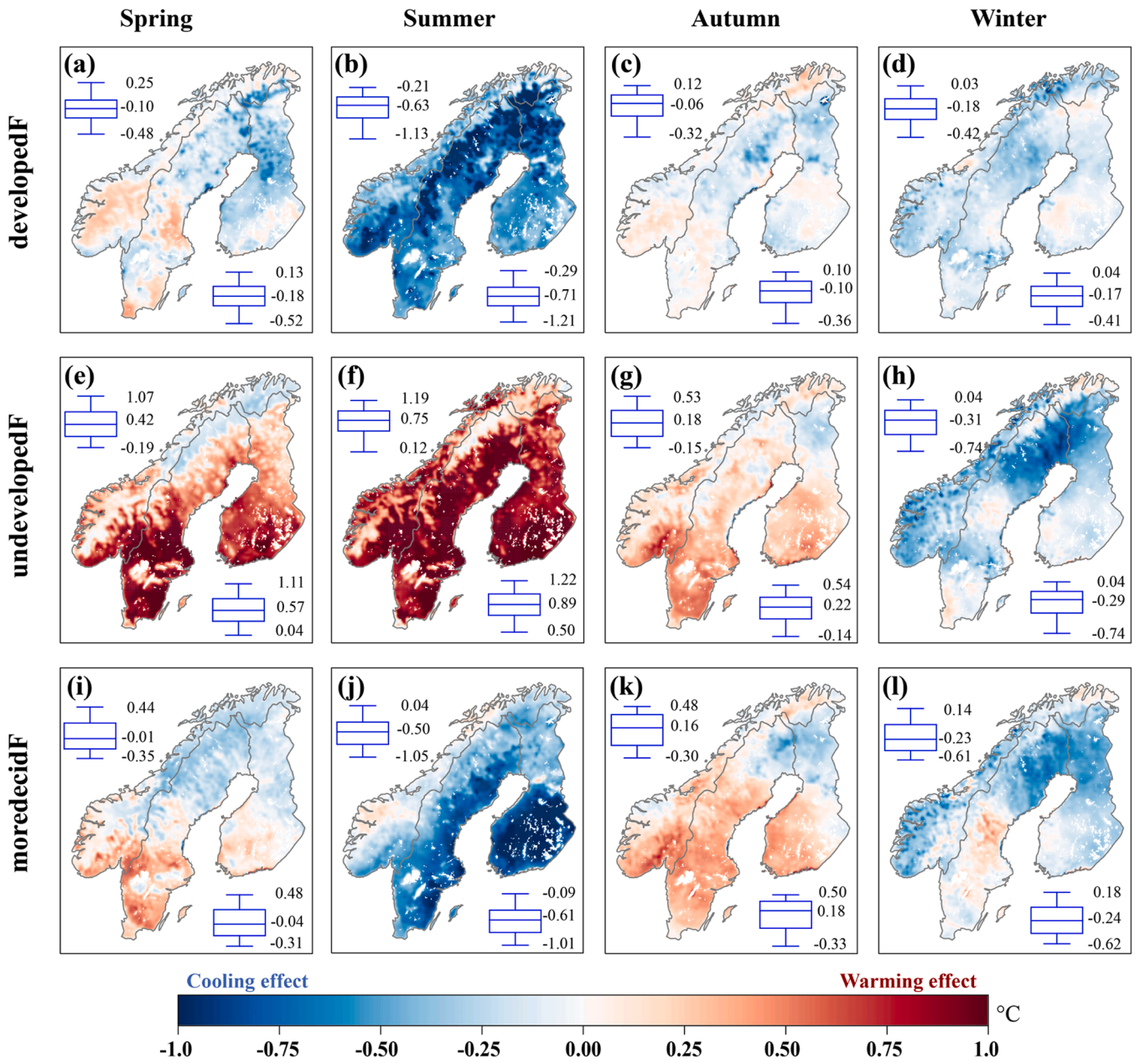

Fig. 4. Seasonal average land surface temperature changes (unit: °C) induced from the investigated forest scenarios including a full development class of all forested areas (developedF; a-d), all undeveloped forests (undevelopedF; e-h), and the transition from evergreen forests to deciduous forests (moredecidF; i-l). Boxplots in the top-left corner show the spatial variability across the land grids in Fennoscandia and in the bottom-right corner show the spatial variability on the grids with forest change (the range indicates the 5th and 95th percentile, the box the standard deviation, the line in the box the mean).

3.4. Decomposition analysis of temperature changes and key drivers

In the developedF scenario, the mean spring cooling in land surface temperature over the affected grids (−0.16 °C, with a range from −0.52 °C to 0.13 °C as the 5th and 95th percentile, Fig. 4) can be mainly attributed to a decrease in sensible heat, an increase in latent heat and less incoming shortwave solar radiation reaching the surface (Fig. 5a and Figure S3 in Supplementary Information). In summer, the mean cooling effect is particularly strong, and it is primarily driven by decreases in incoming shortwave radiation. This can be connected to the higher evapotranspiration rates of mature forests that increase the presence of clouds, which reduce the amount of solar energy reaching the surface. Mean changes are smaller in autumn and winter. For the annual mean changes, the main component is the reduction in shortwave radiation (together with the imbalance term). The seasonal breakdown of the decomposition analysis is available in Table S8.

In the case of undevelopedF, the mean warming in spring is primarily the result of increased sensible heat fluxes and reduced latent heat, which is the outcome of lower vegetation cover (Fig. 5b). A similar result is found in summer and autumn, where all components contribute to warming. In winter, most of the region experiences cooling driven by reduced longwave radiation and soil fluxes. Annually, the land temperature change is mostly positive throughout the domain (Figure S4), and it is primarily dominated by increased sensible heat (Figure S5). As for the developedF case, changes in albedo play a minor role relative to other changes in the different components of the surface energy balance.

In the moredecidF case, there is almost no change in the mean spring land surface temperature across the domain, as there is a balance between moderate warming of approximately 0.1–0.5 °C in southern Norway, Sweden, and Finland, and moderate cooling of about −0.2 to

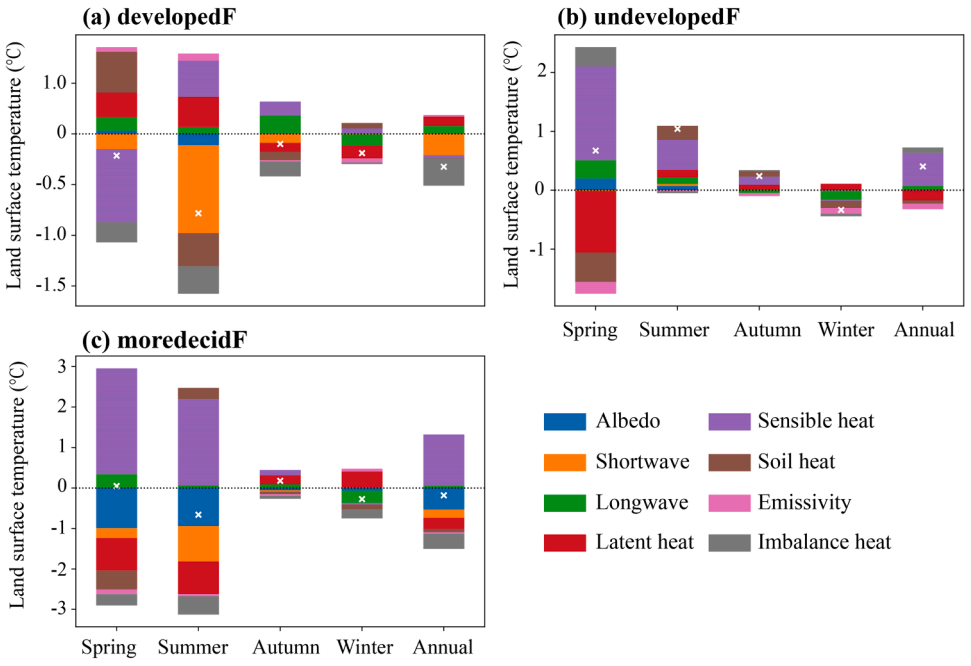

Fig. 5. Decomposition of seasonal, and annual mean land surface temperature (LST) changes (ΔLST, unit: °C) into different factors induced from the investigated forest scenarios, i.e. a full development class of all forested areas (developedF; a), all undeveloped forests (undevelopedF; b), and the transition from evergreen forests to deciduous forests (moredecidF; c). The eight factors include albedo, incoming shortwave radiation, incoming longwave radiation, latent heat flux, sensible heat flux, soil heat flux, emissivity, and surface imbalance heat flux, using the temperature decomposition method. The white cross represents the net change in LST. The height of each bar represents the average magnitude of the change in each factor across the entire domain.

−0.5 °C in other regions (Fig. 4). The decomposition analysis shows that the warming driven by the increase in sensible heat is mainly counterbalanced by a cooling from surface albedo (as deciduous species have a lower snow masking effect than evergreen forests) and reduction in latent heat fluxes (Fig. 5c). In summer, the spatial pattern of the net temperature changes is largely in contrast to what observed in spring (Figure S6), but the decomposition analysis shows similar results. Although of smaller magnitude, the same direction of the individual components of the surface energy budget is observed for the annual mean as well. The situation differs for the results in autumn and winter, but net changes in land surface temperature are small and net variations of the individual components are more limited.

4. Discussion

In this study, we integrate an enhanced forest structure and distribution dataset with a high-resolution regional climate model to investigate the model's capability to capture the direct impacts of alternative forest development stages and composition on regional climate via changes in surface energy balance. Compared to the default land cover classification, an enhanced forest cover product with three different forest development classes and two main tree species (evergreen and

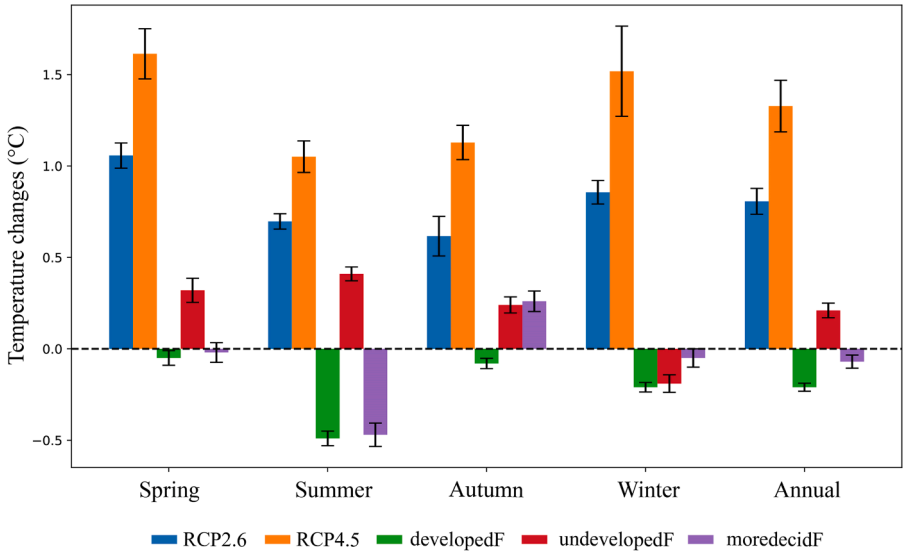

Fig. 6. Comparison of the seasonal and annual mean 2 m air temperature changes between the investigated forest scenarios and the predicted temperature changes between 2010 and 2050 under RCP2.6 and RCP4.5 in Fennoscandia. The uncertainty ranges in the RCPs and forest scenarios represent the standard error in each scenario.

deciduous) showed improved accuracy in reproducing observed 2 m air temperature and land surface temperature, and allowed to explore the temperature response to alternative forest types.

Increasing the presence of more developed and mature forests in Fennoscandia can decrease temperatures throughout the year, particularly during summer. This is mainly attributed to a decrease in incoming shortwave solar radiation induced by changes in cloud cover promoted by higher evapotranspiration rates. The summer-induced cooling is large enough to compensate for about 70 % of the future warming expected in Fennoscandia from the RCP2.6 scenario in 2050 (relative to 2010) (Fig. 6). On an annual basis, the cooling can offset about 25 % of the predicted warming. These relative contributions to a regional mitigation of global warming effects are more reduced in the case of a higher impact scenario such as RCP4.5. In this case, the cooling benefits in the summer correspond to about 47 % of the predicted warming, which becomes 16 % in terms of the annual mean.

The predominance of low-developed and/or early-stage successional forest (undevelopedF) is associated with a warming contribution in summer, spring, autumn, and throughout the year, and it is primarily driven by increased sensible heat due to reductions in evapotranspiration from the decline in vegetation cover. The warming effect in summer is equal to about 60 % of the one expected in Fennoscandia under RCP2.6, and 39 % of the one under RCP4.5. In terms of annual mean temperature changes, the relative importance of the average warming is more moderate, ranging from about 25 % in RCP2.6 to about 16 % in RCP4.5.

A shift in tree species from evergreen to deciduous forests, which can be interpreted as a strategy to promote nature conservation by favouring natural regeneration, induces a decrease in shortwave radiation (as deciduous species have higher evapotranspiration rates, thereby favouring cloud formation), an increase in albedo (as deciduous trees have higher albedo values in summer and a lower snow-masking effects in winter and spring than evergreen species), and an increase in latent heat flux (from higher evapotranspiration rates), resulting in a robust summer cooling. This cooling benefit is about 67 % of the expected warming from RCP2.6, and 45 % in the case of RCP4.5. The cooling effect in the other seasons and the annual mean is more uncertain though, as the regional temperature response is spatially heterogenous and the uncertainty ranges span from negative to positive values. This is maybe due to the multiple effects at play when a change in tree species is simulated, and the net effects on temperature are more dependant on the background climatic conditions.

The simulations with the WRF model coupled to the enhanced land cover classification exhibit a low level of bias and RMSE. The statistical performance indicators are comparable to that of the most common regional climate models used for simulating local-to-regional climate of land cover changes in Europe (Davin et al., 2020; Huang et al., 2020; Kotlarski et al., 2014). Most regional climate model simulations from previous studies typically underestimate annual mean temperature (−2.0 to −0.2 °C) relative to observations in northern Europe (Kotlarski et al., 2014). Past simulations specifically based on the WRF regional climate model show large spread biases in Scandinavia, with a regional underestimation from −2.2 to 1.1 °C in winter, and from −3.0 to −0.13 °C in summer (Kotlarski et al., 2014; Vautard et al., 2021). Our simulations have smaller error ranges for both annual mean (−1.40 °C) and seasonal mean temperature (−0.43 °C for winter and −0.32 °C for summer). Overall, these results demonstrate the advantages of using an enhanced forest cover dataset with more specific parameterization of forests in Fennoscandia for improving the accuracy of regional climate model simulations.

Generally, our findings are consistent with previous observational studies conducted in boreal forests (Alkama and Cescatti, 2016; Lee et al., 2011; Zhang et al., 2014), which indicate that forest clearing tends to increase temperature during summer months, while afforestation has the opposite effect. Our model simulations show effects of forest dynamics that are consistent with other modelling studies investigating the relationship between forest cover and surface temperature, despite the significant diversity in climate system responses exhibited by different climate models. For example, when simulating increased forest cover in Europe, most regional climate models predict widespread cooling (well below −2 °C) during summer, but some models suggest widespread warming (around +2 °C or higher) or even a mixed response (Cherubini et al., 2018; Davin et al., 2020). Within the Scandinavian domain, previous studies based on an individual climate model indicated that expanding forests would lead to additional surface warming during winter and spring (ranging from 1.0 °C to 1.5 °C) and cooling during summer (between −1.6 °C and −1.3 °C) (Cherubini et al., 2018; Hu et al., 2019; Mooney et al., 2021). These studies also suggest that temperature changes are generally smaller in autumn. Although this response is relatively stronger than what we observed in our forest management scenarios, the seasonal trend aligns with our findings. Our study also found similar trends in land surface temperature, although our estimates were lower in magnitude due to the smaller differences in vegetation structure and biomass considered in our forest management scenarios, which involve transitioning from mixed developed forests to either fully developed or under-developed forests. In contrast, previous studies compared temperature differences between forests and open land, either between nearby pairs of sites or before and after afforestation/deforestation, where the changes in vegetation structure are more pronounced. Our study suggests that allowing boreal forests to develop to more mature stages may lead to lower annual mean surface temperatures, mostly driven by cooler summer months, potentially helping to mitigate the effects of summer heat.

There has been limited investigation of the regional climate implications of forests at different development stages in Fennoscandia, hindering the possibility of comparing the main findings from our analysis with previous studies. Consistently with previous research (Alkama and Cescatti, 2016; Naudts et al., 2016; Zhang and Liang, 2018), our decomposition analysis shows that a cooling effect in summer is mainly due to increased evapotranspiration and surface emissivity. Forest development reduces surface albedo, resulting in increased net radiation at the surface and latent and sensible heat fluxes. The partitioning of this extra energy by the vegetation cover determines the extent to which trees increase latent heat flux instead of sensible heat, ultimately leading to cooling effects. Changes in albedo, surface emissivity, and evapotranspiration under varying radiation loads contribute to the seasonal changes in the local climate response to forest dynamics. A previous study based on an offline land surface model shows that more developed forests have a slight annual cooling effect on land surface temperature of 0.04 °C, while undeveloped forests exhibit an annual mean warming of 0.14 °C (Kumkar et al., 2020). Using machine learning-based statistical models, Huang et al. (2023a) found that, compared to the present state of Fennoscandian forests, fully developed forests induce an average cooling of land surface temperature in summer daytime ranging from −0.85 °C to −0.23 °C (depending on the statistical model), with an annual mean warming of 0.26 °C. Conversely, scenarios with undeveloped forests result in an annual average cooling of −0.29 °C but daytime warming in summer that can exceed 1 °C. It is important to note that modelling studies often yield amplified responses compared to observationally constrained estimates (Perugini et al., 2017). These differences can be attributed to variations in the accuracy of land cover representation and physical processes, as modelling studies typically do not optimize physiological properties of the vegetation with their age.

The main unexpected result from our simulations is related to the weak albedo response in winter and spring, which is surprising as the seasonal snow cover should amplify the albedo feedback when reducing (undevelopedF) or maximizing (developedF) forest structure and biomass. This is maybe the reason of the uncommon finding of winter temperature changes in developedF, which shows a slight cooling effect, with land surface temperature showing a decrease of −0.17 ± 0.15 °C and 2 m air temperature of −0.22 ± 0.14 °C. This finding is intriguing considering that an increase in forest structure (especially in LAI) is

typically associated with a reduction in albedo due to the masking effect of snow cover (Anderson et al., 2011; Betts et al., 2007). However, despite the decrease in albedo reported by the model (Supplementary Figure S2), a cooling rather than a warming effect occurs. To further investigate the drivers of these land surface temperature changes, we employed a decomposition method to analyse the contributions of different components. Our analysis revealed the weak temperature effects from albedo changes across all simulations (except for the moredecidF case), and that the changes in temperature in winter and spring are mostly due to changes in moisture fluxes and shortwave radiation. Investigations with other regional climate models could shed light on the extent to which this finding is dependant on an individual model configuration, or it is due to the limited capability of regional climate models to represent internal processes when simulating changes in vegetation phenology of the same tree species that are at different stages of development (instead of contrasting vegetation types, for which validation is more robust). This explanation is maybe supported by the fact that the albedo feedback is more visible when there is a shift from one tree species to another (moredecidF), but not when the same tree species is considered at a different stage of development (despite the structural parameters such as LAI or canopy height are consistently changed). More research can thus aim to improve the representation of the fundamental physical processes of trees along different stages in regional climate models to secure more accurate estimates of the effects of forest management on regional climate.

Impacts of forest cover dynamics on land surface temperature are sometimes found to be more pronounced than those on 2 m air temperature, with changes in land surface temperature being up to 50 % larger than 2 m air temperature, particularly in terms of maximum values. However, the overall patterns and directions of the change remain consistent between the two variables. This finding aligns with observations from satellite-based studies (Alkama and Cescatti, 2016). It is important to note that our approach focuses on estimating regional impacts on temperature resulting from variations in forest structure and land-atmosphere interactions. We have not explicitly accounted for possible large-scale feedback that may arise due to teleconnections, which are long-range atmospheric interactions. These teleconnections could potentially amplify or dampen the regional temperature impacts of forest cover dynamics estimated with regional climate models (Portmann et al., 2022).

Our study focuses on average climatic conditions, thereby disregarding the influence of interannual climate variability. However, the biogeophysical processes driving these temperature changes can exhibit sensitivity to varying background climate conditions from year to year (Li et al., 2016, 2024; Pitman et al., 2011). The evapotranspiration effect is sensitive to soil moisture, which is susceptible to changes during drought periods (Davis et al., 2019; Greiser et al., 2024). The expected increase in drought frequency under climate change can lead to shortages in soil moisture and lower evapotranspiration rates (Seneviratne et al., 2010; von Arx et al., 2013). This means that during dry spells the moisture benefits associated with developed forests may diminish, resulting in decreased evapotranspiration and subsequently lower latent heat fluxes. As a result, the cooling effects typically associated with fully developed forests in summer can be reduced (Brodribb et al., 2020; Li et al., 2024). Notably, factors like snow cover and its duration yield a substantial influence on the surface energy balance and the mechanisms shaping temperature variations. In warmer years, the presence and duration of snow cover diminish, thereby reducing the significance of the albedo mechanism. Elevated winter temperatures lead to shortened snow cover duration and reduced depth, ultimately diminishing the cooling impact attributable to snow's reflective properties on harvested areas. The reduction in the snow-albedo cooling effect has the potential to reduce the biogeophysical temperature cooling associated to forest harvest activities in the region (Wei et al., 2022).

5. Conclusions

The use of an enhanced forest cover product in an up-to-date regional climate model can improve model performance in reproducing 2 m air temperature and land surface temperature, and it facilitates the investigation of the effects on regional climate of alternative forest development stages and composition that are indicative of different forest management strategies. An expansion of the predominance of mature and/or fully developed forests in Fennoscandia as advocated to maximize vegetation carbon stocks has the potential to exert a regional biogeophysical cooling with reductions in both land surface and 2 m air temperature, especially in the summer. This cooling benefit is primarily attributed to reduced incoming shortwave radiation, resulting from an increase in cloud cover triggered by enhanced evapotranspiration fluxes from the increased vegetation. On the other hand, the predominance of undeveloped or early-successional forests induces an annual mean increase in temperature, especially in summer, primarily due to increased sensible heat fluxes driven by a reduction in evapotranspiration caused by the simplification of the vegetation cover. Furthermore, a transition from evergreen to deciduous forests, a proxy for a typical management strategy aiming at promoting natural regeneration for nature conservation, results in a less certain annual average cooling effect (-0.07 ± 0.19 °C), which is mainly due to changes in surface albedo, and to a more robust summer cooling. Overall, these simulations show that an extensive change in the forest development stage can induce a temperature effect that corresponds to a significant fraction of the expected warming by 2050 (from 16 % to 70 %, depending on the specific scenario-RCP combination and season). As the effective implementation of alternative management practices will be more gradual and nuanced than what simulated here, these temperature changes likely represent a theoretical maximum. However, they provide an indication of the direction that regional temperature effects can take if deploying practices that either increase or decrease forest structure or favour a tree species change towards a higher presence of deciduous trees. Overall, these results can be generally explained by a temperature decomposition analysis and by comparison with previous studies, although some findings are unexpected (e.g., cooling effects in winter of a fully developed forest). Simulations with other RCMs and more research at the interface between observations and modelling are needed to constraint existing uncertainties on the influence of forest dynamics on regional climate.

Increasing the understanding of the importance of the connections between forestry and the regional climate can help to inform resource managers and authorities about the consequences of changes in harvest intensities or tree species (e.g., from evergreen to deciduous species) beyond a mere carbon accounting perspective, providing a more holistic view on the climate change mitigation opportunities connected with forest management. Only considering carbon fluxes and overlooking biogeophysical temperature implications can lead to the identification of sub-optimal practices and miss opportunities for potential synergies between global climate change mitigation and regional implementation with co-benefits for adaptation (e.g., potential mitigation of summer warming). Any large-scale change in management practices requires social acceptability and political support for financial resources, which can be facilitated by considering multi-criteria approaches and integrated strategies that can optimize climate change mitigation along with other environmental aspects, such as biodiversity, sustainable resource management, and socio-economic benefits for local communities.

Open research

Data availability statement

The source code for the regional climate model (WRF v4.3) can be found on the wrf-model GitHub repository (https://github.com/wrf-model/WRF, accessed on September 20, 2023) (Skamarock et al., 2021). The ESA CCI land cover classification map and model validation

datasets E-OBS (Cornes et al., 2018) and ERA5-Land (Muñoz-Sabater et al., 2021) are available for download from the Climate Data Store (https://cds.climate.copernicus.eu/, accessed on September 21, 2023). The enhanced forest data is sourced from the Norwegian Institute of Bioeconomy Research (NIBIO) (https://bird.unit.no/resources/10,261,768-feb9-4c37-8c08-ea2efe5342ef, accessed on September 21, 2023) (Majasalmi et al., 2018). The CORDEX regional climate model simulations are available from the ESFG platform (https://esgf-data.dkrz.de/search/cordex-dkrz/, accessed on February 28, 2024). For access to the model simulation data used to generate figures in the manuscript and supplementary information via Zenodo repository (https://zenodo.org/record/8,365,723, accessed on September 21, 2023) (Huang et al., 2023b).

CRediT authorship contribution statement

Bo Huang: Writing – review & editing, Writing – original draft, Visualization, Validation, Investigation, Formal analysis, Data curation. **Yan Li:** Writing – review & editing, Validation, Investigation. **Xia Zhang:** Writing – review & editing, Investigation. **Chunping Tan:** Writing – review & editing, Validation, Investigation. **Xiangping Hu:** Writing – review & editing, Methodology, Investigation. **Francesco Cherubini:** Writing – review & editing, Supervision, Investigation, Funding acquisition, Conceptualization.

Declaration of competing interest

The authors declare that they have no known competing financial interests or personal relationships that could have appeared to influence the work reported in this paper.

Data availability

The data has been shared in Zenodo repository (https://zenodo.org/record/8,365,723)

Acknowledgements

B.H., X.H., and F.C. acknowledge the support of the Norwgian Research Council (project no. 286773, 294534, and 288047). Y. L. acknowledges the support from the China Scholarship Council (CSC). C.T. thanks the support of the National Natural Science Foundation of China (Grant No. 42201085) and the Regional Innovation Joint Research Program of Sichuan Province (Grant No. 2023YFQ0105). Simulations were performed on the resources provided by UNINETT Sigma2—the National Infrastructure for High Performance Computing and Data Storage in Norway.

Supplementary materials

Supplementary material associated with this article can be found, in the online version, at doi:10.1016/j.agrformet.2024.110083.

References

Alkama, R., Cescatti, A., 2016. Biophysical climate impacts of recent changes in global forest cover. Science 351 (6273), 600–604.
Ameray, A., Bergeron, Y., Valeria, O., Girona, M.M., Cavard, X., 2021. Forest carbon management: a review of silvicultural practices and management strategies across boreal, temperate and tropical forests. Curr. For. Rep. 7 (4), 245–266.
Anderson, R.G., et al., 2011. Biophysical considerations in forestry for climate protection. Front. Ecol. Environ. 9 (3), 174–182.
Betts, R.A., 2000. Offset of the potential carbon sink from boreal forestation by decreases in surface albedo. Nature 408 (6809), 187–190.
Betts, R.A., Falloon, P.D., Goldewijk, K.K., Ramankutty, N., 2007. Biogeophysical effects of land use on climate: model simulations of radiative forcing and large-scale temperature change. Agr Forest Meteorol 142 (2–4), 216–233.
Bonan, G.B., 2008. Forests and climate change: forcings, feedbacks, and the climate benefits of forests. Science 320 (5882), 1444–1449.
Brodribb, T.J., Powers, J., Cochard, H., Choat, B., 2020. Hanging by a thread? Forests and drought. Science 368 (6488), 261–266.
Cherubini, F., Huang, B., Hu, X.P., Tölle, M.H., Stromman, A.H., 2018. Quantifying the climate response to extreme land cover changes in Europe with a regional model. Environ. Res. Lett. 13 (7), 074002.
Cornes, R.C., van der Schrier, G., van den Besselaar, E.J.M., Jones, P.D., 2018. An ensemble version of the E-OBS temperature and precipitation data sets. J Geophys Res-Atmos 123 (17), 9391–9409.
Crowther, T.W., et al., 2015. Mapping tree density at a global scale. Nature 525 (7568), 201–205.
Davin, E.L., et al., 2020. Biogeophysical impacts of forestation in Europe: first results from the LUCAS (Land Use and Climate Across Scales) regional climate model intercomparison. Earth Syst Dynam 11 (1), 183–200.
Davis, K.T., Dobrowski, S.Z., Holden, Z.A., Higuera, P.E., Abatzoglou, J.T., 2019. Microclimatic buffering in forests of the future: the role of local water balance. Ecography. 42 (1), 1–11.
De Frenne, P., et al., 2021. Forest microclimates and climate change: importance, drivers and future research agenda. Glob. Chang. Biol. 27 (11), 2279–2297.
De Frenne, P., et al., 2019. Global buffering of temperatures under forest canopies. Nat. Ecol. Evol. 3 (5), 744–749.
de Noblet-Ducoudré, N., et al., 2012. Determining robust impacts of land-use-induced land cover changes on surface climate over North America and Eurasia: results from the first set of LUCID experiments. J Climate 25 (9), 3261–3281.
Doughty, C.E., et al., 2018. Tropical forest leaves may darken in response to climate change. Nat. Ecol. Evol. 2 (12), 1918–1924.
Duveiller, G., Hooker, J., Cescatti, A., 2018. The mark of vegetation change on Earth's surface energy balance. Nat. Commun. 9 (1), 679.
Ellison, D., et al., 2017. Trees, forests and water: cool insights for a hot world. Global Environ. Chang. 43, 51–61.
ESA, 2017. Land Cover CCI product user guide version 2. https://maps.elie.ucl.ac.be/CCI/viewer/download/ESACCI-LC-Ph2-PUGv2_2.0.pdf (Accessed 27 May 2022).
Greiser, C., et al., 2024. Higher soil moisture increases microclimate temperature buffering in temperate broadleaf forests. Agr. Forest Meteorol 345.
Haesen, S., et al., 2023. ForestClim-Bioclimatic variables for microclimate temperatures of European forests. Glob. Chang. Biol. 29 (11), 2886–2892.
Hansen, M.C., et al., 2013. High-resolution global maps of 21st-century forest cover change. Science 342 (6160), 850–853.
Hausfather, Z., Peters, G.P., 2020. Emissions - the 'business as usual' story is misleading. Nature 577 (7792), 618–620.
Hersbach, H., et al., 2020. The ERA5 global reanalysis. Quart. J. Royal Meteorolog. Soc. 146 (730), 1999–2049.
Högberg, P. et al., 2021. Sustainable boreal forest management challenges and opportunities for climate change mitigation.
Hu, X.P., Huang, B., Cherubini, F., 2019. Impacts of idealized land cover changes on climate extremes in Europe. Ecol. Indic. 104, 626–635.
Huang, B., et al., 2020. Predominant regional biophysical cooling from recent land cover changes in Europe. Nat. Commun. 11 (1), 1066.
Huang, B., et al., 2023a. A simplified multi-model statistical approach for predicting the effects of forest management on land surface temperature in Fennoscandia. Agr Forest Meteorol 332, 109362.
Huang, B., et al., 2023b. Investigating the local temperature response to forest management with a regional climate model. Zenodo.
Iacono, M.J., et al., 2008. Radiative forcing by long-lived greenhouse gases: calculations with the AER radiative transfer models. J Geophys Res-Atmos 113, D13103.
Iordan, C.M., Hu, X., Arvesen, A., Kauppi, P., Cherubini, F., 2018. Contribution of forest wood products to negative emissions: historical comparative analysis from 1960 to 2015 in Norway, Sweden and Finland. Carbon. Balance Manage 13 (1), 12.
Jackson, R.B., et al., 2008. Protecting climate with forests. Environ. Res. Lett. 3 (4), 044006.
Kain, J.S., 2004. The Kain-Fritsch convective parameterization: an update. J. Appl. Meteorol 43 (1), 170–181.
Katragkou, E., et al., 2015. Regional climate hindcast simulations within EURO-CORDEX: evaluation of a WRF multi-physics ensemble. Geosci. Model. Dev. 8 (3), 603–618.
Kellomäki, S., Väisänen, H., Kirschbaum, M.U.F., Kirsikka-Aho, S., Peltola, H., 2021. Effects of different management options of Norway spruce on radiative forcing through changes in carbon stocks and albedo. Forestry 94 (4), 588–597.
Komatsu, H., Kume, T., 2020. Modeling of evapotranspiration changes with forest management practices: a genealogical review. J Hydrol 585, 124835.
Kotlarski, S., et al., 2014. Regional climate modeling on European scales: a joint standard evaluation of the EURO-CORDEX RCM ensemble. Geosci. Model. Dev. 7 (4), 1297–1333.
Kumkar, Y., Astrup, R., Stordal, F., Bright, R.M., 2020. Quantifying regional surface energy responses to forest structural change in nordic fennoscandia. J Geophys Res-Atmos 125 (15), e2019JD032092.
Lawrence, D.M., et al., 2019. The community land model version 5: description of new features, benchmarking, and impact of forcing uncertainty. J. Adv. Model Earth Sy 11 (12), 4245–4287.
Lawrence, D.M., et al., 2011. Parameterization Improvements and Functional and Structural Advances in Version 4 of the Community Land Model. J Adv Model Earth Sy 3, M03001.
Lee, X., et al., 2011. Observed increase in local cooling effect of deforestation at higher latitudes. Nature 479 (7373), 384–387.
Li, Y., et al., 2016. The role of spatial scale and background climate in the latitudinal temperature response to deforestation. Earth Syst. Dynam. 7 (1), 167–181.

Li, Y., Huang, B., Rust, H.W., 2024. Using statistical models to depict the response of multi-timescale drought to forest cover change across climate zones. Hydrol. Earth Syst. Sci. 28 (2), 321–339.
Lu, Y.Q., Kueppers, L.M., 2012. Surface energy partitioning over four dominant vegetation types across the United States in a coupled regional climate model (Weather Research and Forecasting Model 3-Community Land Model 3.5). J. Geophys Res.-Atmos 117, D06111.
Luyssaert, S., et al., 2014. Land management and land-cover change have impacts of similar magnitude on surface temperature. Nat. Clim. Change 4 (5), 389–393.
Luyssaert, S., et al., 2018. Trade-offs in using European forests to meet climate objectives. Nature 562 (7726), 259–262.
Majasalmi, T., Eisner, S., Astrup, R., Fridman, J., Bright, R.M., 2018. An enhanced forest classification scheme for modeling vegetation-climate interactions based on national forest inventory data. Biogeosciences. 15 (2), 399–412.
Mäkelä, A., et al., 2023. Effect of forest management choices on carbon sequestration and biodiversity at national scale. Ambio 52 (11), 1737–1756.
McGrath, M.J., et al., 2015. Reconstructing European forest management from 1600 to 2010. Biogeosciences. 12 (14), 4291–4316.
Mooney, P.A., Lee, H., Sobolowski, S., 2021. Impact of quasi-idealized future land cover scenarios at high latitudes in complex terrain. Earths. Future 9 (2), e2020EF001838.
Mooney, P.A., Sobolowski, S., Lee, H., 2020. Designing and evaluating regional climate simulations for high latitude land use land cover change studies. Tellus A 72 (1), 1853437.
Muñoz-Sabater, J., et al., 2021. ERA5-Land: a state-of-the-art global reanalysis dataset for land applications. Earth. Syst. Sci. Data 13 (9), 4349–4383.
Nakanishi, M., Niino, H., 2006. An improved mellor-yamada level-3 model: its numerical stability and application to a regional prediction of advection fog. Boundary. Layer. Meteorol. 119 (2), 397–407.
Naudts, K., et al., 2016. Europe's forest management did not mitigate climate warming. Science (1979) 351 (6273), 597–600.
Oke, T., 1987. Boundary Layer Climates, 2nd edition. Routledge, London and New York.
Oleson, K. et al., 2013. Technical description of version 4.5 of the community land model (CLM). NCAR Technical Note NCAR/TN-503+STR: 169.
Oleson, K.W. et al., 2010. Technical description of version 4.0 of the community land model (CLM). NCAR/TN-478+STR.
Pan, Y., et al., 2011. A large and persistent carbon sink in the world's forests. Science 333 (6045), 988–993.
Perugini, L., et al., 2017. Biophysical effects on temperature and precipitation due to land cover change. Environ. Res. Lett. 12 (5), 053002.
Petersson, H., et al., 2022. On the role of forests and the forest sector for climate change mitigation in Sweden. Gcb Bioenergy 14 (7), 793–813.
Pitman, A.J., et al., 2011. Importance of background climate in determining impact of land-cover change on regional climate. . Clim. Change 1 (9), 472–475.
Portmann, R., et al., 2022. Global forestation and deforestation affect remote climate via adjusted atmosphere and ocean circulation. Nat. Commun. 13 (1), 5569.
Seneviratne, S.I., et al., 2010. Investigating soil moisture-climate interactions in a changing climate: a review. Earth-Sci. Rev. 99 (3–4), 125–161.
Skamarock, W.C. et al., 2021. A description of the advanced research WRF model version 4.3. NCAR Tech. Note NCAR/TN–556+STR.
Thompson, G., Field, P.R., Rasmussen, R.M., Hall, W.D., 2008. Explicit forecasts of winter precipitation using an improved bulk microphysics scheme. Part II: implementation of a new snow parameterization. Mon. Weather. Rev. 136 (12), 5095–5115.
Vautard, R., et al., 2021. Evaluation of the large EURO-CORDEX regional climate model ensemble. J. Geophys Res.-Atmos 126 (17), e2019JD032344.
Venäläinen, A., et al., 2004. Simulations of the influence of forest management on wind climate on a regional scale. Agr. Forest Meteorol 123 (3–4), 149–158.
von Arx, G., Pannatier, E.G., Thimonier, A., Rebetez, M., 2013. Microclimate in forests with varying leaf area index and soil moisture: potential implications for seedling establishment in a changing climate. J. Ecol. 101 (5), 1201–1213.
Wei, X.H., et al., 2022. Forest harvesting and hydrology in boreal Forests: under an increased and cumulative disturbance context. Forest Ecol. Manag. 522, 120468.
Winckler, J., Reick, C.H., Bright, R.M., Pongratz, J., 2019. Importance of surface roughness for the local biogeophysical effects of deforestation. J. Geophys. Res.-Atmos 124 (15), 8605–8618.
Zhang, M., et al., 2014. Response of surface air temperature to small-scale land clearing across latitudes. Environ. Res. Lett. 9 (3), 034002.
Zhang, Y.Z., Liang, S.L., 2018. Impacts of land cover transitions on surface temperature in China based on satellite observations. Environ. Res. Lett. 13 (2), 024010.
Zhou, N., et al., 2021. Overview of recent land cover changes, forest harvest areas, and soil erosion trends in Nordic countries. Geogr. Sustain 2 (3), 163–174.